



HAL
open science

A necrotic cell death model in a protist

C. Laporte, A. Kosta, G. Klein, L. Aubry, D. Lam, E. Tresse, M. F. Luciani,
P. Golstein

► **To cite this version:**

C. Laporte, A. Kosta, G. Klein, L. Aubry, D. Lam, et al.. A necrotic cell death model in a protist. Cell Death and Differentiation, 2007, 14 (2), pp.266-274. 10.1038/sj.cdd.4401994 . hal-00165463

HAL Id: hal-00165463

<https://hal.science/hal-00165463v1>

Submitted on 28 Sep 2023

HAL is a multi-disciplinary open access archive for the deposit and dissemination of scientific research documents, whether they are published or not. The documents may come from teaching and research institutions in France or abroad, or from public or private research centers.

L'archive ouverte pluridisciplinaire **HAL**, est destinée au dépôt et à la diffusion de documents scientifiques de niveau recherche, publiés ou non, émanant des établissements d'enseignement et de recherche français ou étrangers, des laboratoires publics ou privés.

A necrotic cell death model in a protist

C Laporte^{1,2,3}, A Kosta^{1,2,3}, G Klein⁴, L Aubry⁴, D Lam^{1,2,3}, E Tresse^{1,2,3}, MF Luciani^{1,2,3} and P Golstein^{*,1,2,3}

While necrotic cell death is attracting considerable interest, its molecular bases are still poorly understood. Investigations in simple biological models, taken for instance outside the animal kingdom, may benefit from less interference from other cell death mechanisms and from better experimental accessibility, while providing phylogenetic information. Can necrotic cell death occur outside the animal kingdom? In the protist *Dictyostelium*, developmental stimuli induced in an autophagy mutant a stereotyped sequence of events characteristic of necrotic cell death. This sequence included swift mitochondrial uncoupling with mitochondrial 2',7'-dichlorofluorescein diacetate fluorescence, ATP depletion and increased oxygen consumption. This was followed by perinuclear clustering of dilated mitochondria. Rapid plasma membrane rupture then occurred, which was evidenced by time-lapse videos and quantified by FACS. Of additional interest, developmental stimuli and classical mitochondrial uncouplers triggered a similar sequence of events, and exogenous glucose delayed plasma membrane rupture in a nonglycolytic manner. The occurrence of necrotic cell death in the protist *Dictyostelium* (1) provides a very favorable model for further study of this type of cell death, and (2) strongly suggests that the mechanism underlying necrotic cell death was present in an ancestor common to the *Amoebozoa* protists and to animals and has been conserved in evolution.

Cell Death and Differentiation (2007) 14, 266–274. doi:10.1038/sj.cdd.4401994; published online 30 June 2006

Different types of cell death have long been defined in morphological terms.^{1,2} Thus, mammalian cells can die from 'apoptosis', 'necrosis' and 'autophagic cell death', and intermediate or mixed cell death types have also been reported. While caspase-dependent apoptosis has been studied in detail, less is known regarding the precise molecular mechanisms underlying caspase-independent types of cell death. These may play an important role especially in pathological circumstances and are thus now attracting considerable interest. Caspase-independent cell death mechanisms that are not prominent in the usual model organisms may be more experimentally accessible in simpler biological models,³ with potentially less interference from other cell death pathways. The underlying mechanisms may be phylogenetically conserved, which would be of interest in itself and would allow the extension of results obtained with simple models to higher eukaryotes.

In animal cells, necrosis is often defined as a nonapoptotic, nonautophagic type of cell death, with swelling of cells and organelles and, importantly, early plasma membrane rupture.^{4,5} At a molecular level, necrosis but not apoptosis is often accompanied by acute ATP depletion that is thought to cause cell death.^{6,7}

Dictyostelium discoideum, a protist that emerged in evolution after plants and from an ancestor common to fungi and animals,⁸ shows developmental cell death.⁹ This can be mimicked in monolayers of *Dictyostelium* cells subjected to starvation and to the differentiation-inducing factor DIF-1 (hereafter designated DIF¹⁰). The type of cell death thus

obtained includes vacuolization.^{11,12} Vacuolization is dependent on autophagy as inactivation of the *atg1* autophagy gene¹³ prevented it. Importantly, when subjected to starvation and DIF, these *atg1-1* cells still died, but now of a rapid nonvacuolar cell death.¹⁴

We report here that this nonvacuolar cell death in *Dictyostelium* possesses classical characteristics of necrotic cell death. This strongly suggests that the mechanism underlying necrotic cell death emerged in evolution before the divergence to *Amoebozoa* protists and animals.

Results

Rapid mitochondrial uncoupling. Hallmarks of necrotic cell death in mammalian cells include a rapid oxidative burst, mitochondrial uncoupling and plasma membrane rupture. To investigate whether early events following the addition of DIF to *Dictyostelium* HMX44A.*atg1-1* cells ('cells', used throughout, unless mentioned otherwise) included an oxidative burst, we used the fluorescent probe 2',7'-dichlorofluorescein diacetate (DC-FDA). Upon addition of DIF, starved cells stained fluorescent in the presence of DC-FDA, as shown by microscopy and by flow cytometry (Figure 1). The same pattern of fluorescent labelling was obtained with dihydrorhodamine 123 and aminophenyl fluorescein, but not with hydroethidium or MitoSOX Red (not shown). Like other signs of nonvacuolar cell death, DC-FDA fluorescence required prior starvation (not shown) and

¹Centre d'Immunologie de Marseille-Luminy, Université de la Méditerranée, Case 906, Parc Scientifique de Luminy, 13288 Marseille Cedex 9, France; ²INSERM U631, 13288 Marseille Cedex 9, France; ³CNRS UMR6102, 13288 Marseille Cedex 9, France and ⁴CEA-Grenoble/DRDC/BBSI, UMR 5092 CNRS-CEA-UJF, 17, rue des Martyrs, 38054 Grenoble Cedex 09, France

*Corresponding author: P Golstein, Centre d'Immunologie de Marseille-Luminy, Case 906, Parc Scientifique de Luminy, 13288 Marseille Cedex 9, France.

Tel: + 33-4-91-26-94-68; Fax: + 33-4-91-26-94-30; E-mail: golstein@ciml.univ-mrs.fr

Keywords: cell death; necrosis; *Dictyostelium*; ATP; mitochondria; glucose

Abbreviations: CCCP, carbonyl cyanide 3-chlorophenylhydrazone; DC-FDA, 2',7'-dichlorofluorescein diacetate; DIF, differentiation-inducing factor; DNP, dinitrophenol; 2-DOG, 2-deoxyglucose; PI, propidium iodide; VDAC, voltage-dependent anion channel

Received 29.3.06; revised 21.4.06; accepted 11.5.06; Edited by JA Cidlowski; published online 30.6.06

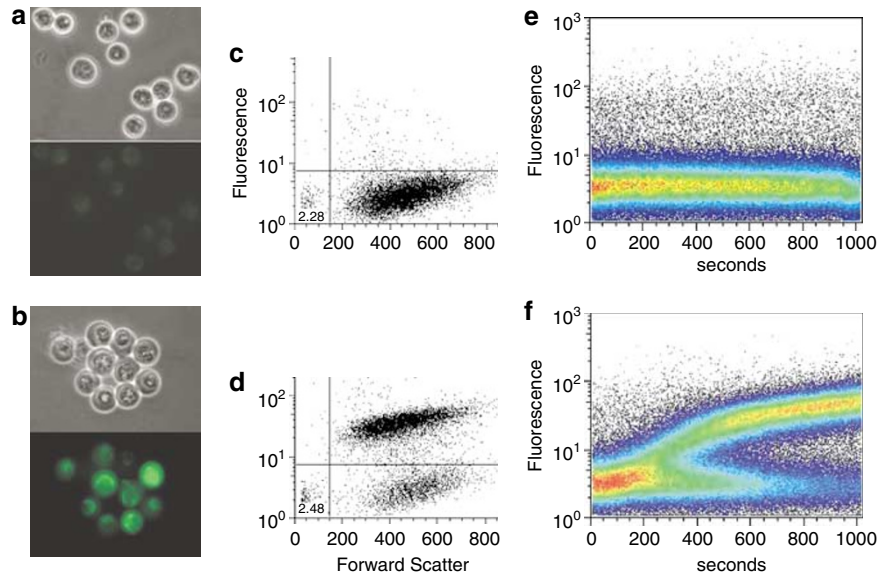


Figure 1 Induction of DC-FDA fluorescence following the addition of DIF. Starved *HMX44A.atg1-1* cells were incubated with DC-FDA and with (b) or without (a) DIF for 15–30 min and analyzed by phase-contrast and fluorescence microscopy. The majority of cells were markedly fluorescent and showed perinuclear clustering of organelles only when DIF was added. Contrast and luminosity had to be increased to see the very weak fluorescence label of cells without DIF. Also, some photoactivation in DC-FDA-labelled cells occurred during fluorescence microscopy examination, leading to an increase in fluorescence only in cells that were already labelled, thus only among DIF-induced cells, therefore not affecting qualitative evaluation of labelling. (c, and d) Flow cytometry showed compared to cells without DIF (c) the presence of a ‘cloud’ of fluorescent cells upon addition of DIF (d). (e, and f) The emergence of fluorescent cells as a function of time was followed by continuous flow cytometry, starting the acquisition immediately after DIF addition. Cells without DIF remained negative (e), whereas after the addition of DIF some cells became fluorescent as soon as 200 s, and most were fluorescent after 1000 s (f)

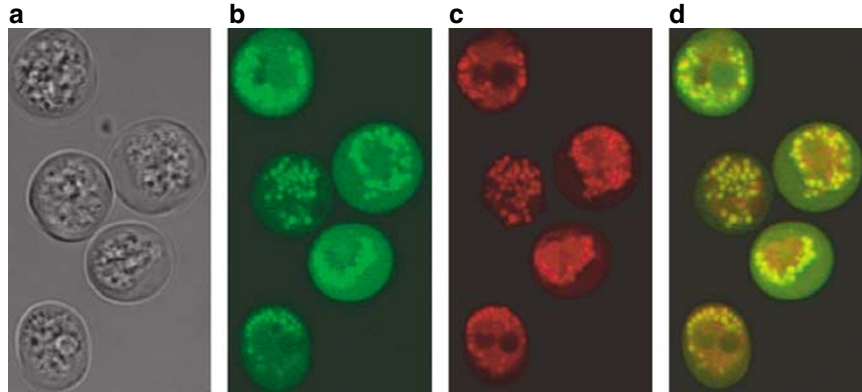


Figure 2 DC-FDA fluorescence is mitochondrial. Cells were observed about 30 min after the simultaneous addition of DIF, DC-FDA and MitoTracker Orange. (a) DIC microscopy, (b) DC-FDA fluorescence, (c) MitoTracker Orange fluorescence and (d) merge b and c

addition of DIF. Remarkably, as shown by flow cytometry some of the DC-FDA-exposed cells became fluorescent within 3 min after the addition of DIF and most of them were fluorescent after 15 min (Figure 1 and not shown). After a few minutes, only few cells with intermediate fluorescence levels could be detected (Figure 1d and f), indicating a rapid transition from no to full fluorescence in each cell. Confocal microscopy of cells after DIF addition showed for most stained structures colocalization of MitoTracker Orange (leading to red fluorescence of mitochondria) and DC-FDA (leading to green fluorescence), indicating that DC-FDA fluorescence was mitochondrial (Figure 2).

The fluorescence of DC-FDA and of dihydrorhodamine 123 is most often interpreted as revealing an oxidative burst, and it

has been argued that oxidative stress can trigger necrotic cell death. However, we did not observe any inhibition of DC-FDA fluorescence and of membrane rupture by an extensive range of inhibitors of oxidative burst (not shown). This might be owing to limited membrane permeability in starved *Dictyostellium* cells (but see also for reservations as to interpretation of DC-FDA fluorescence¹⁵). This lack of effect of inhibitors prevented us from formally concluding on the existence of an oxidative burst early in this cell death pathway. In any case, this DC-FDA fluorescence revealed early DIF-induced events in mitochondria, presumably an oxidative burst, contemporary with mitochondrial uncoupling as shown below.

Unlike apoptotic cell death, mammalian necrotic cell death is often associated with ATP depletion.^{4,6,7} In wild-type

Dictyostelium cells, starvation led to some ATP depletion, which was not increased upon addition of DIF; this may be related to the absence of increased DC-FDA fluorescence in this case (not shown). In *atg1-1* cells, starvation similarly led to ATP depletion. This apparent ATP depletion upon starvation in both parental and *atg1-1* cells may merely result from a starvation-induced reduction in size occurring in both types of cells. However, in starved *atg1-1* but not in wild-type cells, ATP per cell was further decreased upon addition of DIF (Figure 3a), likely through a decrease of the cellular concentration of ATP. Significant ATP depletion occurred within 3 min after the addition of DIF (Figure 3b). This ATP depletion suggested that DIF could directly or indirectly uncouple mitochondrial oxidative phosphorylation. An immediate consequence of such uncoupling should be an increase in oxygen consumption rate, which indeed occurred within less than a minute after the addition of DIF (or of dinitrophenol (DNP) as a positive control showing mitochondrial uncoupling) to starved cells (Figure 3c). We conclude that addition of DIF to starved cells leads to almost immediate uncoupling of mitochondrial oxidative phosphorylation.

About 20 min after the addition of DIF, some cells became round with perinuclear clustering of cell organelles, which extended to almost all cells by 30 min (time-lapse videos in Online Supplementary Material). By electron microscopy, most cells showed at this time perinuclear clustering of otherwise dilated mitochondria.¹⁴ Clustering may be linked to the dependence of the actin system on energy supply by ATP. Perinuclear clustering has been reported also in circum-

stances other than necrotic cell death, while dilation of mitochondria is usually associated with it.

Plasma membrane rupture. In animal cells, one of the most distinctive traits of necrotic cell death compared to other types of cell death is rapid rupture of the plasma membrane. In wild-type *Dictyostelium* cells, 50% of the cells showed membrane rupture about 36 h after the addition of DIF, as detected by propidium iodide (PI) uptake.^{11,12} In *atg1-1* cells, this occurred 30–300 min after the addition of DIF as shown by phase-contrast microscopy (Figure 4) and by time-lapse videos (Online Supplementary Material). Sequences of still frames from these videos allowed a more precise timing of the duration of the membrane rupture event itself. Only about 15 s were required to shift from an apparently intact plasma membrane to its almost complete disappearance (Figure 4a). In some but not all instances, an increase in apparent cell volume could be detected just before membrane rupture (time-lapse videos in Online Supplementary Material). This cell swelling and the mitochondrial swelling seen by electron microscopy¹⁴ are reminiscent of the classical cell and organelle swelling in mammalian necrotic cell death.

In all cases, plasma membrane rupture left behind some 'core' material (Figure 4a) whose aspect was distinct from that of the initial living cell. This physical change of dying cells suggested that detection and quantification of this cell death might be possible through measure of cell scatter. Indeed, flow cytometry showed upon addition of DIF the appearance of events of lower forward scatter (FSC) and slightly higher side scatter (SSC), generating a 'cloud' distinct from that of

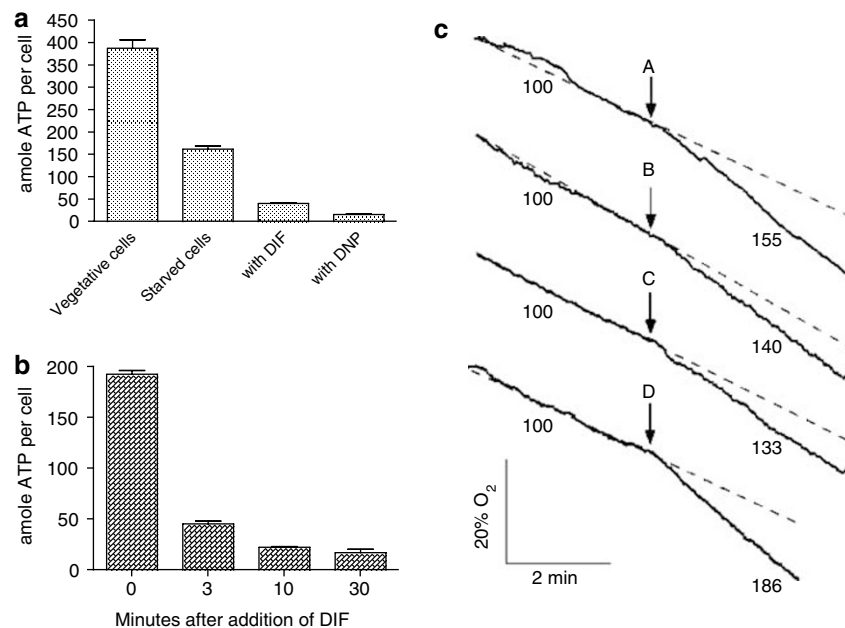


Figure 3 Mitochondrial uncoupling following the addition of DIF. **(a)** Stepwise ATP depletion in HMX44A.*atg1-1* cells after starvation and incubation with DNP or DIF. Cells were either grown in HL5 medium (vegetative cells) or incubated overnight in MES buffer (starved cells). The latter cells were also incubated for 30 min with 100 nM DIF or 100 μ M DNP. Perchloric cellular extracts were then prepared for determination of ATP levels per cell. Each column shows mean attomoles ATP per cell \pm S.E.M. of sextuplicate samples. **(b)** DIF induced most of the ATP depletion within 3 min as shown by the amount of ATP present in extracts from starved cells prepared 0, 3, 10 or 30 min after DIF addition. **(c)** Increase in oxygen consumption rates upon addition of DNP or DIF. At the times indicated by arrows, DNP (A, 100 μ M) or DIF (B, 100 nM; C, 250 nM; D, 500 nM) was added to starved *atg1-1* cells, which led within less than a minute to an increase in oxygen consumption rate. Values below the traces indicate oxygen consumption rates as percentages of the rate before additions (indicated by the dashed line)

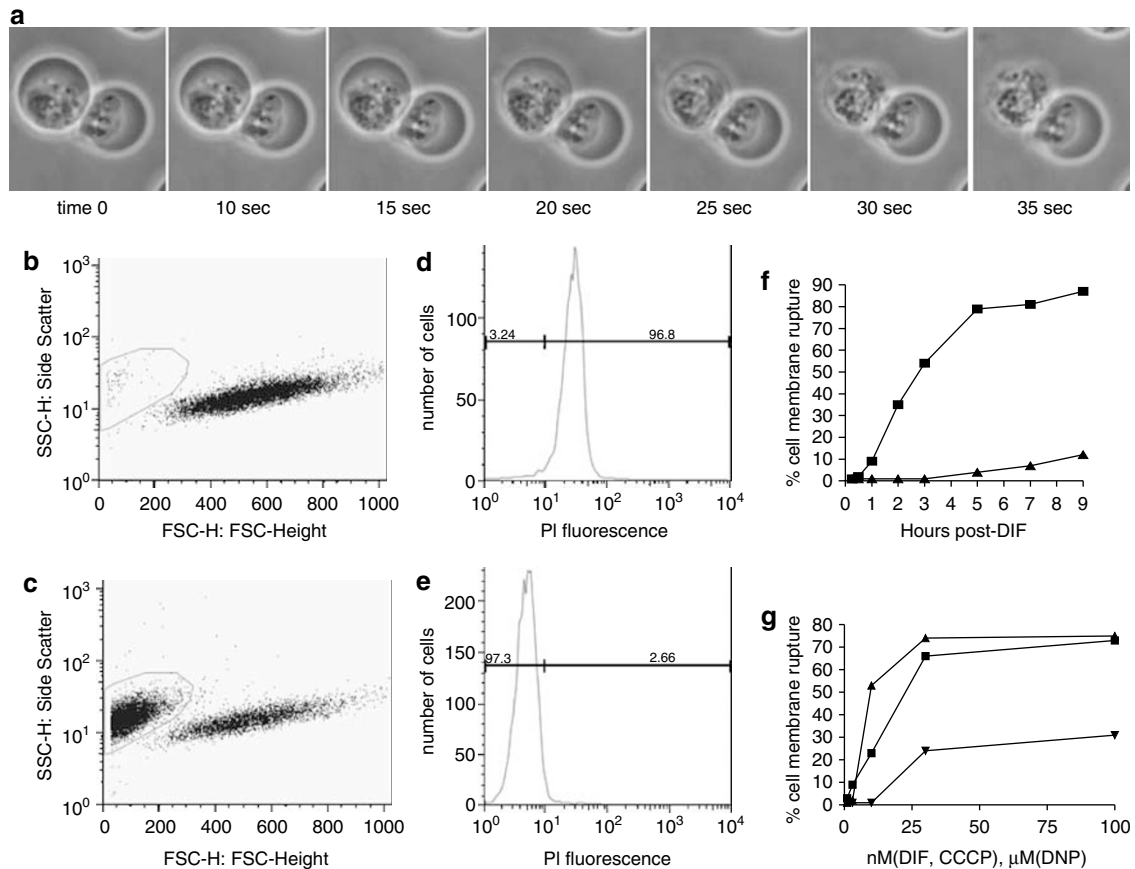


Figure 4 Membrane rupture following the addition of DIF or classical mitochondrial uncouplers. (a) Starved HMX44A. *atg1-1* cells were subjected to time-lapse movies following the addition of DIF. A sequence of still frames extracted from time-lapse video 7 (in Online Supplementary Material) shows two cells 2 h after the addition of DIF, of which one shows rupture of its external membrane between the 20 s and the 35 s time points. (b and c) Detection and quantification by FACS of cell membrane rupture. FACS output of forward versus SSC of HMX44A. *atg1-1* cells, (b) without DIF or (c) 2.5 h after the addition of DIF. The latter shows a newly appeared ‘cloud’ of cells with ruptured membrane. (d and e) PI check of the proportion of dead cells in the cell clouds obtained by FACS (as in c). Before FACS analysis, cell populations were labelled with PI, which would only label cells with altered plasma membrane. (d) Cells from the cloud appearing after the addition of DIF were 97% positive, and (e) Cells from the pre-existing cloud were only 3% positive. (f) In another experiment, the percentage of cells in the newly appeared cloud in (c) that is, the percentage of cells dead according to the criterion of membrane rupture, could be followed with time after the addition of DIF; ▲, without DIF; ■, with DIF. (g) Percentage of starved cells with membrane rupture as a function of the concentrations of DIF (▼), DNP (▲) or CCCP (■), 2.5 h after their addition, a time when the percentage cell membrane rupture for DIF-induced death, is not maximal and varies significantly from experiment to experiment. This percentage would rise further at later times, reaching a maximum around 5 h post-DIF (see f)

cells not subjected to DIF (Figure 4b and c). Cells in the cloud appearing after the addition of DIF were dead, as 96–98% were positive for PI staining compared to 2–4% in the pre-existing cloud (Figure 4d and e). Within the time frame of these experiments, no gross secondary degradation of dead cells occurred that might generate a high proportion of large debris counted as new dead cells, as judged by relative stability of dead cell ‘cloud’ parameters and by microscopy (not shown). As an additional check, in every experiment we systematically verified the state of cells by phase-contrast microscopy, and found a consistent and strong correlation between the degree of cell alteration seen at 60 min post-DIF and the % cell membrane rupture measured by FACS at 2.5 h post-DIF.

Flow cytometry of unlabelled cells thus allowed quantitative assessment of the proportion of dead cells, for instance, at various times after the addition of DIF (Figure 4f). While without DIF cell death remained below 15% even at 9 h, upon addition of DIF cell death reached a maximum of more than

75% after 5 h. Half-maximum values were reached at 2.5 h post-DIF, which was therefore used thereafter as a sensitive read-out time. The slope of the curve at this time indicated a speed of cell death of about 20% cells per hour (Figure 4f), a useful indication in time-lapse experiments that statistically one cell out of five would die in a given microscope field within 1 h. In this report, we operationally define cell death as rupture of the cell membrane, resulting under the microscope in a smaller and immobile mass of mostly organelles or organelle remnants, which can be stained by PI and shows by flow cytometry a shift in scatter.

As shown above, DIF induces uncoupling of oxidative phosphorylation and plasma membrane rupture. Addition of the classical inducers of uncoupling DNP or carbonyl cyanide 3-chlorophenylhydrazone (CCCP) to starved (but not to unstarved) cells also led to ATP depletion and oxygen consumption increase, DC-FDA fluorescence, perinuclear clustering, and early plasma membrane rupture (Figures 3 and 4g and not shown). Both latter traits were also observed in

parental cells (not shown). This similar effect of dissimilar molecules all endowed with uncoupling activity indicated that in starved cells mitochondrial uncoupling may be sufficient for subsequent events including plasma membrane rupture. We then wished to investigate how this uncoupling can lead to plasma membrane rupture.

From mitochondrial uncoupling to membrane rupture, as probed with exogenous glucose. In mammalian cells, ATP depletion linked to uncoupling is often believed to be the cause of necrotic cell death, on the basis of results showing that provision of glucose led to both replenishment of ATP and prevention of necrotic cell death in mammalian cells.^{6,7,16–18} To try to link mitochondrial uncoupling and membrane rupture in *Dictyostelium* necrotic cell death, we investigated whether exogenous glucose would both prevent or delay cell death and replenish ATP, in this system in which

the cells were deprived of glucose because of experimental starvation and *atg1* mutation.

The addition of 5 mM glucose indeed delayed DIF-induced cell death as assessed by membrane rupture (Figure 5a) by more than 6 h, thus increasing more than fourfold the time required to reach a given level of cell death. The addition of glucose to *atg1-1* cells (but not to parental cells, not shown) led to markedly less membrane rupture at 2.5 h after DIF in each of more than 30 experiments. The addition of glucose did not, however, prevent or grossly delay DC-FDA fluorescence (Figure 5b), showing that exogenous glucose affected a cell death stage downstream of mitochondrial events. DIF-induced glucose-delayed cell death was morphologically similar to that occurring earlier in the absence of glucose (not shown). Glucose delayed plasma membrane rupture induced not only by DIF but also by classical uncouplers (Figure 5c). The delay in membrane rupture observed

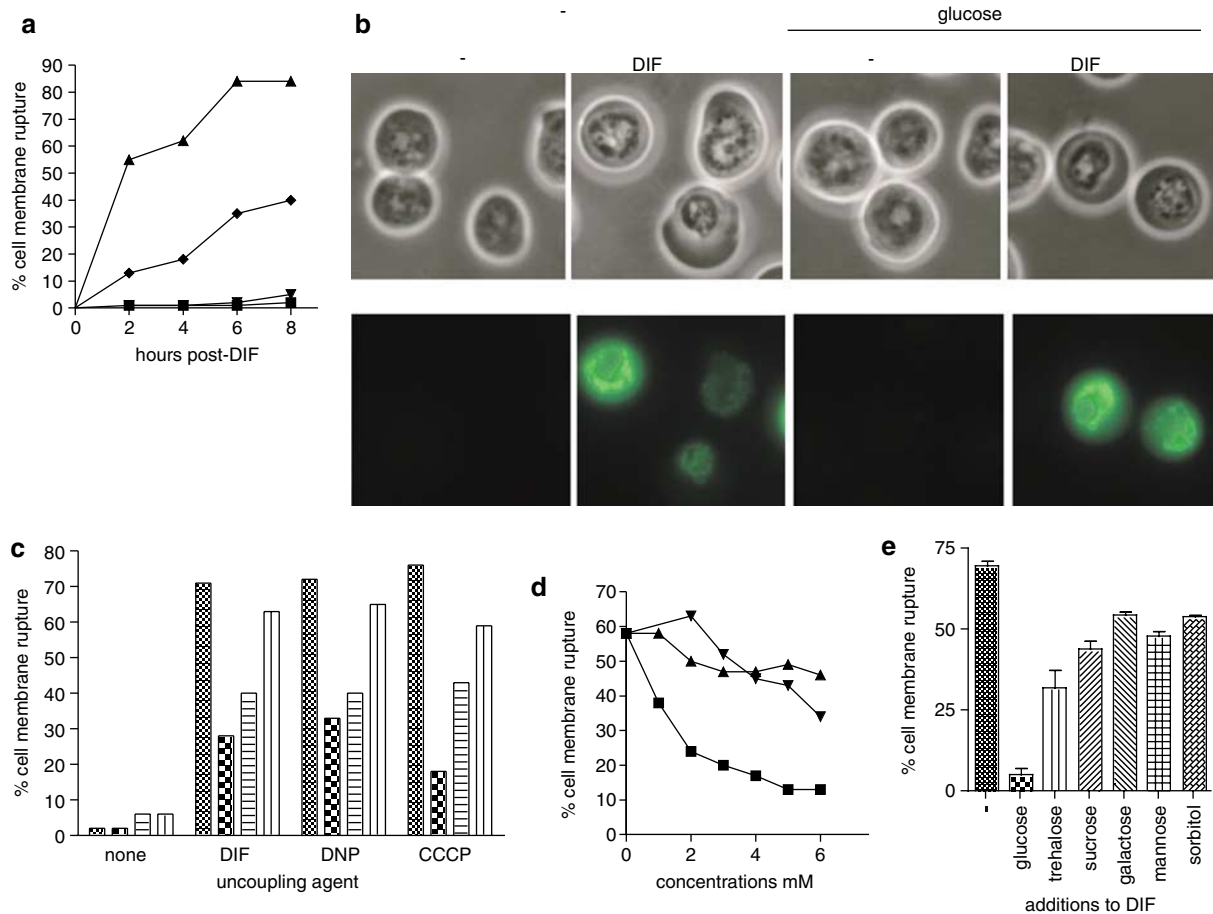


Figure 5 Glucose but not some other sugars delays cell membrane rupture. (a) Glucose slowed down DIF-induced cell membrane rupture. Starved HMX44A. *atg1-1* cells were incubated with DIF in the absence (▲) or in the presence of 5 mM glucose (◆), and the percentage of cells with membrane rupture was followed with time. Controls without DIF with (■) or without glucose (▼) showed almost no death. (b) Glucose did not grossly delay DIF-induced DC-FDA fluorescence or perinuclear clustering. Starved cells were incubated for 30 min in the presence of glucose 5 mM. Then, without discarding glucose, DC-FDA was added together with, or without DIF, and cells were checked by microscopy after another 30 min. All fluorescent pictures were taken with a set exposure time of 2 s. In each labelled cell, organelles form a fluorescent cluster around a much smaller nucleus. (c) Also uncoupler-induced cell membrane rupture is delayed by glucose or 2-DOG but not by sorbitol. Starved cells were preincubated for 30 min with no sugar, or 5 mM of glucose, 2-DOG or sorbitol (from left to right in each group of four columns, respectively), then in some chambers 100 nM of DIF, or 30 μ M of DNP, or 30 nM of CCCP, or no uncoupler, was added as indicated. Cell membrane rupture was checked 2.5 h after this addition. (d) Glucose delays cell membrane rupture more than fructose or sorbitol. Starved cells were incubated for 30 min in the absence or in the presence of 1–6 mM of glucose (■), fructose (▲) or sorbitol (▼), then without removing the sugars DIF was added. Percentage cell membrane rupture was measured by flow cytometry after 2.5 h of incubation. (e) Glucose delays cell membrane rupture more than each of a range of sugars and than sorbitol. Starved cells were incubated for 30 min in the absence or in the presence of 5 mM of the indicated sugar, and treated as in (d)

with exogenous glucose was not, or far less, observed with 5 mM sorbitol or fructose (Figure 5d), thus excluding a simple osmotic effect. Also, trehalose and to a lesser extent sucrose, known to confer more efficiently than glucose cell resistance to an abiotic stress possibly through peculiar solution properties (for a review see Crowe *et al.*¹⁹), were far less efficient than glucose at delaying membrane rupture (Figure 5e), making this explanation unlikely in the present situation.

Although glucose delayed DIF-induced plasma membrane rupture, in marked contrast addition of galactose or mannose led to no more membrane rupture delay than the sorbitol control (Figure 5e). This showed that specific recognition of glucose was required for its membrane effect. 6-Deoxyglucose led to little membrane rupture delay (Figure 6a), showing that C6 is significant for the delaying effect of glucose. Importantly, 2-deoxyglucose (2-DOG), that can be C6-phosphorylated but cannot undergo glycolysis past this phosphorylation, led to a delay in DIF (and also DNP and CCCP)-induced membrane rupture (Figures 5c and 6a, c), however sometimes less marked than with glucose. This result showed that at least part of the membrane-rupture-delaying effect of glucose can occur without glycolysis. Consistent with the 2-DOG results, addition of glucose 5 mM did not obviously replenish ATP (Figure 6b) tested 5–120 min after addition of DIF (not shown). In contrast, addition as a control of cell-permeant methylpyruvate replenished ATP or prevented its depletion (Figure 6b) and also prevented DIF-induced DC-FDA fluorescence, perinuclear clustering (not shown) and membrane rupture (Figure 6c). Altogether, in *Dictyostelium* necrotic cell death exogenous glucose delayed membrane rupture otherwise than through glycolysis and ATP replenishment, strongly indicating a nonglycolytic effect of glucose in this case.

Discussion

Necrotic cell death: from mitochondrial uncoupling to cell membrane rupture. Following addition of DIF to starved *atg1-1Dictyostelium* cells, early events occurring within 1–3 min include DC-FDA mostly mitochondrial fluorescence, ATP depletion and oxygen consumption increase, all of these pointing toward mitochondrial uncoupling. This is consistent with the fact that DIF can be replaced by the classical uncouplers DNP or CCCP. These results are complementary to those of Shaulsky and Loomis,²⁰ who showed that DIF was able to reduce the membrane potential of isolated submitochondrial particles. Both sets of results lead to the conclusion that there is an uncoupling effect of DIF. The results of Shaulsky and Loomis²⁰ indicated that the uncoupling effect of DIF may occur through its direct interaction with mitochondria. Thus, remarkably the DIF differentiation factor may act at least in part through rapid uncoupling of oxidative phosphorylation.

In *Dictyostelium* development, DIF has also been shown to activate transcription factors. When added after a 4 h starvation period, DIF led within 2–3 min to the tyrosine phosphorylation of the STATc transcription factor,²¹ thus detectably preventing the exit of STATc from the nucleus,²² and induced changes in subcellular localization of the transcription factor DimB.^{23,24} The relationship between DIF-induced rapid phosphorylation events and DIF-induced rapid uncoupling of oxidative phosphorylation is not known.

The fact that distinct moieties such as DNP and CCCP (classical uncouplers) and DIF induced both mitochondrial uncoupling and plasma membrane rupture strongly indicated that in this system mitochondrial uncoupling is sufficient for membrane rupture. Whether there is a causal relationship between ATP depletion and membrane rupture could not be

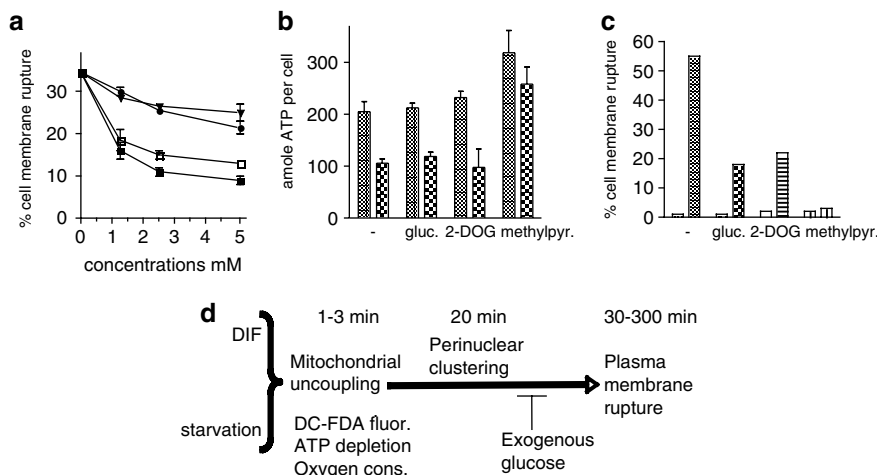


Figure 6 Further characteristics of glucose-mediated delay of membrane rupture. (a) Effect of glucose (■), sorbitol (▼), 2-DOG (open square) or 6-deoxyglucose (filled circle) on cell membrane rupture. Cells were treated as in Figure 5d. (b) Glucose or 2-DOG do not replenish ATP, whereas methylpyruvate prevents ATP depletion. Starved cells were preincubated for 30 min with no sugar, or 5 mM of glucose, 2-DOG or methylpyruvate as indicated, then in some chambers DIF was added (right column of each group of two). The amount of ATP per cell was measured 30 min after the addition of DIF. (c) Glucose but also 2-DOG and methylpyruvate delay cell membrane rupture. Starved cells were incubated for 30 min in the absence or in the presence of 5 mM glucose, 2-DOG or methylpyruvate as indicated, then DIF was added in some chambers (right column in each group of two). Percentage cell membrane rupture was measured by flow cytometry after 2.5 h of incubation. (d) Schematic representation of the *Dictyostelium* necrotic cell death model. Starved *atg1-1* cells to which the differentiation factor DIF is added undergo mitochondrial uncoupling. This is sufficient for subsequent plasma membrane rupture as shown by the effect of classical uncouplers. The addition of exogenous glucose delays plasma membrane rupture in a nonglycolytic manner

investigated in this system using glucose, because glucose affected membrane rupture otherwise than by replenishing ATP. Thus, mitochondrial uncoupling seems sufficient to ensure plasma membrane rupture, but it is not known whether this is through ATP depletion (although ATP depletion is a convenient explanation for alterations of the cytoskeleton leading to perinuclear clustering of mitochondria, and of membrane ATP-dependent molecular pumps contributing to membrane rupture).

Plasma membrane rupture delayed by glucose. In mammalian necrotic cell death, glucose-induced rescue was explained through concomitant ATP replenishment.^{6,7} In *Dictyostelium* necrotic cell death, addition of glucose or of 2-DOG led to membrane rupture delay with no ATP replenishment (this report). At least in *Dictyostelium*, factors other than ATP depletion govern membrane rupture in necrotic cell death, and can be controlled by exogenous glucose. In mammalian necrotic cell death, these factors may occur, but may have been ignored owing to the readily available explanation of ATP replenishment through glycolysis.

Exogenous glucose may act *extracellularly* to stabilize the membrane, either by a direct effect or through transmembrane signaling by unspecified glucose receptors. Exogenous glucose may also, or instead, act *intracellularly*, which we tend to favor based on the requirement for C6 phosphorylation and on the commonly accepted intracellular location of hexokinases/glucokinases. Once in cells, to delay membrane rupture glucose must be both specifically recognized and C6-phosphorylated, presumably by a glucokinase. *Dictyostelium* possesses no hexokinases but structurally unrelated glucokinases (Eichinger *et al.*²⁵; see also <http://dictybase.org/>), which, of note, showed activity in cells undergoing development.²⁶ Glucose delayed plasma membrane rupture but not DC-FDA fluorescence, perinuclear clustering of mitochondria or ATP depletion. Thus, the delaying effect of glucose was downstream or independent of early mitochondrial events.

The efficacy of 2-DOG and the absence of ATP replenishment strongly indicate that the effect of glucose on membrane rupture was not through glycolysis. In animal cells, glucose can modulate hexokinases in an energy-independent manner leading to voltage-dependent anion channel control of mitochondria, thereby affecting apoptotic cell death.^{27–30} Also, in some animal cells glucose inhibited cell death apparently through the pentose phosphate pathway.³¹ As an example, some mammalian cells could be protected from H₂O₂-induced necrotic cell death by 2-DOG flowing into the pentose phosphate pathway and producing NADPH; exogenous glucose led only or mostly to glycolysis, and the pentose phosphate pathway was favored only when 2-DOG was added instead of glucose.³² In starved *Dictyostelium* cells, for unknown reasons exogenous glucose cannot undergo glycolysis. In both cases, (Le Goffe *et al.*³², this report), ATP was not produced.

Altogether, we conclude that mitochondrial uncoupling leads to plasma membrane rupture in this necrotic cell death, whereas exogenous glucose delays it nonglycolytically (Figure 6d).

***Dictyostelium* necrotic cell death and the phylogenesis of cell death.**

Dictyostelium, a protist, belongs to the unikont group of eukaryotes together with fungi and animals.³³ The present results show that a similar necrotic cell death pathway can operate in both animal cells and *Dictyostelium*. Necrosis would thus seem more widespread and more ancient than apoptosis dependent on *bona fide* caspases, which is restricted to the animal kingdom. Necrosis must have existed in an ancestor common to *Dictyostelium* and animals, and may thus qualify as a primordial cell death mechanism within unikont eukaryotes. It will be of interest to check whether a similar necrotic cell death mechanism exists among eukaryotes in other unikonts such as fungi, and in bikonts such as plants.

The existence of several distinct types of cell death coexisting in the same cell (for a review see Golstein and Kroemer³⁴) raises the question of which selective advantage led to their emergence in evolution. This bears on phylogenetic evolution of a function, as opposed to that of a molecule or of a species. In phylogeny, a primordial (necrotic) cell death mechanism may have been conserved through at least some eukaryotic kingdoms. This conservation of necrotic cell death may have been accompanied by serial addition of molecules allowing other types of cell death, for instance, caspases at the emergence of the animal kingdom to allow apoptosis, perhaps initially to facilitate cell corpse dismantling.³⁴

More specifically, in a remote ancestor of *Dictyostelium*, a primordial necrotic mechanism of cell death may have operated upon starvation, possibly on some isolated cells to ensure survival of others. Addition upon evolution of *atg1* and autophagy would have allowed initial developmental aggregation (which *atg1-1* mutant cells cannot undergo³⁵). It would have led also to a much slower course of cell death in *Dictyostelium* (compare the kinetics of death for *atg1-1* cells in this report and for wild-type cells¹¹). A slower course of cell death during *Dictyostelium* development would have provided enough time in this development for morphogenetic signalling of prestalk to prespore cells, cellulose synthesis and formation of a stalk. This may be an example of evolutionary modulation of cell death (interestingly, modulation of mechanism rather than of occurrence) inducing/allowing a shift in developmental pattern.

A model for the study of necrotic cell death. *Dictyostelium* stalk cell death, at least as mimicked in monolayer cultures, is triggered by DIF and starvation, which are physiological stimuli of *Dictyostelium* development. This cell death is autophagic vacuolar for parental cells and necrotic for *atg1-1* cells. Thus, *Dictyostelium* cell death (Kosta *et al.*¹⁴; this report) is necrotic when autophagy is prevented, reminiscent of mouse embryonic interdigital cell death being necrotic when apoptosis is prevented,³⁶ providing examples of necrotic cell death resulting from developmental signals at least when other cell death mechanisms are inhibited.

Necrotic death of *atg1-1 Dictyostelium* cells is one of the very few instances where a developmental trigger leads in a cell line to death in the absence of genes encoding bcl-2 family members, or caspase or metacaspase genes (its only paracaspase gene is not involved in cell death³⁷ and Lam

et al., in preparation). This cell line can undergo neither autophagy nor apoptosis, thus ensuring minimal interference from other types of cell death with its necrotic cell death. *Dictyostelium* bears a haploid and now sequenced genome, which contributes to its experimental and genetic tractability. Together with a few other thoroughly studied models (for instance, mammalian cells^{4,38} and *Caenorhabditis elegans*⁵), this model is thus attractive for further investigation on molecular mechanisms of necrotic cell death.

Materials and Methods

Cells, cell culture and light microscopy. *D. discoideum* axenic strains HMX44A (for derivation, see Levraud *et al.*¹²) and HMX44A. *atg1-1* (an HMX44A derivative mutated for the autophagy gene *atg1*¹⁴) were routinely grown at 22°C in HL5 medium³⁹ as modified,¹¹ except for maltose which was 9 g/l. Blasticidin (10 µg/ml) was added to the HMX44A.*atg1-1* cultures.

For experiments, unless stated otherwise, vegetative cells in growth phase were washed once and resuspended in 10 mM MES (MES hydrate, Sigma M2933) prepared in demineralized water. The pH of this MES buffer was found to matter. The pH < 6 increased, and pH > 6.6 decreased cell membrane rupture, perinuclear clustering and DC-FDA fluorescence (not shown). The pH was therefore adjusted at 6.4 with NaOH in all experiments, and every molecular species tested in this report was checked not to alter this pH by more than 0.2 pH Units. The cells were adjusted at a concentration of 3×10^5 cells/ml. One milliliter of this cell suspension was distributed in each well of Lab-Tek culture chambers (ref. 155380, Nalge Nunc, Naperville, IL, USA; these have a thin glass coverslip bottom allowing high-power inverted fluorescence microscopy) with the addition of cAMP to a final concentration of 3 mM. Incubation proceeded for 16 h at 22°C in MES buffer and cAMP. The previously used 8 h incubation period^{11,40} was found limiting for *atg1-1* cells. A starvation period of sufficient duration was essential for efficient induction by DIF of necrotic cell death. Cells were then washed once by careful removal and addition of MES and incubated at 22°C in either MES, or MES in the presence of the differentiation factor DIF-1 (DN1000, Affiniti Research Products, Exeter, UK) at a final concentration of 10^{-7} M, unless stated otherwise (varying the concentrations of DIF did not modify the type of death but changed it quantitatively: when tested at 7 h post-DIF, percentage cell membrane rupture and perinuclear clustering induced by 10^{-7} M DIF dropped by about 50% at 3×10^{-8} M, and was almost not detectable at 10^{-8} M). After incubation for the indicated period of time, cells in the Lab-Tek chambers were examined using an inverted Zeiss Axiovert 200 microscope usually with a $\times 100$ oil-immersion objective. Pictures were taken using an AxioCam MRC digital camera connected to a PC equipped with Axiovision (Zeiss). In some cases, pictures were taken using a confocal microscope (Zeiss Axiovert 200, LSM510) with a $\times 63$ oil immersion objective, with the scanning module at 1024 \times 1024 pixel resolution, 8 bits, using a scan average of 4, and Argon/2 and HeNe1 lasers with BP 505–530 and LP 560 filters. Images were analyzed with LSM software using false colors. Images and time-lapse videos were transferred to a Macintosh computer and treated with Graphic Converter. Figure assemblies were carried out using FreeHand and Illustrator.

Measurement of cell membrane rupture. Flow cytometry enables to quantify the proportion of cells with a disrupted membrane. Cells in Lab-Tek chambers were resuspended and transferred to tubes and data acquisition was performed on a FACScan cytometer with CELLQuest software (Becton Dickinson) for FSC and SSC parameters, which allowed to distinguish cells with a disrupted membrane from those with an intact one. To exclude debris, an FSC threshold was applied based on the light properties of the cells populations in FSC and SSC modes. Five thousand or 10 000 events were collected per sample. Data analysis was performed with CELLQuest software. In some experiments, cells were labelled with PI (1 µg/ml, Sigma) for 10 min before FACS cytometry.

Measurement of fluorescence possibly revealing production of reactive oxygen species. Possible production of reactive oxygen species was assessed by microscopy and flow cytometry analysis. For each point of analysis, cells were incubated for 15 min at room temperature, protected from light, with either 2',7'-DC-FDA (10 µM, Sigma-Aldrich) or dihydrorhodamine 123 (1 µM, Sigma-Aldrich). For microscopy, cells in Lab-Tek culture chambers were examined directly after incubation by microscopy using Filter set 09 (Zeiss) for 2',7'-DC-FDA

and Filter set 15 (Zeiss) for dihydrorhodamine 123. For flow cytometry, data acquisition was performed directly after incubation, on a FACScan cytometer with CELLQuest software (Becton Dickinson) using FL1 filter. For acquisitions as a function of time, we used a time resolution of 1 s. Data were analyzed using FlowJo software (Tree Star Inc.). To assess mitochondrial localization of DC-FDA fluorescence, cells were incubated with DIF, DC-FDA 10 µM and MitoTracker Orange (Molecular Probes) 500 nM in Lab-Tek chambers for 20 min and observed under the confocal microscope. Pictures were taken between 20 and 40 min after DIF addition.

Measurement of ATP Levels. ATP measurements were performed on 1 ml of cell suspension (5×10^5 cells/ml). Cells were lysed by three sonications of 5 s (3W, Ultrasonic Processor, Bioblock Scientific) on ice, immediately followed by the addition of perchloric acid 70% (125 µl for 1 ml of cell suspension), mixing and centrifugation at 4°C for 5 min at 14 000 r.p.m. The supernatant was then collected in a new tube and pH was adjusted to 7.0 with potassium hydroxide 8 N. After 30 min on ice and 10 min centrifugation at 4°C at 14 000 r.p.m., the supernatant was collected in a new tube. The supernatant could be stored at -20°C for later measurement. ATP levels present in the cellular extract was measured with ATP assay mix (FLAAM, Sigma) by luminometry. Results were expressed as amount of ATP per cell.

Measurement of oxygen consumption. Cells were starved overnight in 10 mM Mes-Na buffer, pH 6.4. in the presence of cAMP. Aliquots (1×10^7 cells) were then collected by centrifugation, resuspended in 2 ml of Mes-Na buffer and transferred to a thermostated oxygraphic cell fitted with a Clark oxygen electrode. Oxygen consumption was recorded as a function of time.

Incubation with sugars. Given sugars were added to starved cells in Lab-Tek chambers, at the indicated final concentrations, 30 min before the addition of DIF or of DNP or CCCP. Sugars were: D-(+)-glucose (Merck 1.083770250 or Sigma G 7528; these batches gave the same results), D-(-)-fructose (Sigma F 3510), D-(+)-galactose (Sigma G 0750), D-(+)-mannose (Fluka 63579), D-sorbitol (Sigma S 3889), sucrose (Sigma S 0389), trehalose (Sigma T 0299), 2-deoxy-D-glucose (Sigma D 6134) and 6-deoxy-D-glucose (Sigma D 9761). After the indicated duration of incubation, cells were checked by microscopy and/or by flow cytometry.

Acknowledgements. We thank INSERM and CNRS for institutional support, and for specific grants Agence Nationale pour la Recherche (DictyDeath ANR-05-BLAN-0333-01), the European Community (FP6 STREP TransDeath LSHG-CT-2004-511983), the Ministère pour la Recherche (ACI BCMS174), Cancéropôle PACA and Association pour la Recherche contre le Cancer. We thank Jonathan Ewbank, Didier Marguet, Pierre-Henri Puech and Gérard Brandolin for helpful discussions and reading the manuscript.

1. Kerr JFR, Wyllie AH, Currie AR. Apoptosis: a basic biological phenomenon with wide-ranging implications in tissue kinetics. *Br J Cancer* 1972; **26**: 239–257.
2. Clarke PGH, Clarke S. Historic apoptosis. *Nature* 1995; **378**: 230.
3. Golstein P, Aubry L, Levraud JP. Cell-death alternative model organisms: why and which? *Nat Rev Mol Cell Biol* 2003; **4**: 798–807.
4. Lemasters JJ. Dying a thousand deaths: redundant pathways from different organelles to apoptosis and necrosis. *Gastroenterology* 2005; **129**: 351–360.
5. Syntichaki P, Tavernarakis N. The biochemistry of neuronal necrosis: rogue biology? *Nat Rev Neurosci* 2003; **4**: 672–684.
6. Leist M, Single B, Castoldi AF, Kühnle S, Nicotera P. Intracellular adenosine triphosphate (ATP) concentration: a switch in the decision between apoptosis and necrosis. *J Exp Med* 1997; **185**: 1481–1486.
7. Eguchi Y, Shimizu S, Tsujimoto Y. Intracellular ATP levels determine cell death fate by apoptosis or necrosis. *Cancer Res* 1997; **57**: 1835–1840.
8. Baldauf SL, Roger AJ, Wenk-Siefert I, Doolittle WF. A kingdom-level phylogeny of eukaryotes based on combined protein data. *Science* 2000; **290**: 972–977.
9. Whittingham WF, Raper KB. Non-viability of stalk cells in *Dictyostelium*. *Proc Natl Acad Sci USA* 1960; **46**: 642–649.
10. Kay RR. Cell differentiation in monolayers and the investigation of slime mold morphogens. *Methods Cell Biol* 1987; **28**: 433–448.
11. Cornillon S, Foa C, Davoust J, Buonavista N, Gross JD, Golstein P. Programmed cell death in *Dictyostelium*. *J Cell Sci* 1994; **107**: 2691–2704.
12. Levraud JP, Adam M, Luciani MF, de Chastellier C, Blanton RL, Golstein P. *Dictyostelium* cell death: early emergence and demise of highly polarized paddle cells. *J Cell Biol* 2003; **160**: 1105–1114.

13. Otto GP, Wu MY, Kazgan N, Anderson OR, Kessin RH. Macroautophagy is required for multicellular development of the social amoeba *Dictyostelium discoideum*. *J Biol Chem* 2003; **278**: 17636–17645.
14. Kosta A, Roisin-Bouffay C, Luciani MF, Otto GP, Kessin RH, Golstein P. Autophagy gene disruption reveals a non-vacuolar cell death pathway in *Dictyostelium*. *J Biol Chem* 2004; **279**: 48404–48409.
15. Halliwell B, Whiteman M. Measuring reactive species and oxidative damage *in vivo* and in cell culture: how should you do it and what do the results mean? *Br J Pharmacol* 2004; **142**: 231–255.
16. Lieberthal W, Menza SA, Levine JS. Graded ATP depletion can cause necrosis or apoptosis of cultured mouse proximal tubular cells. *Am J Physiol* 1998; **274** (Part 2): F315–F327.
17. Leist M, Single B, Naumann H, Fava E, Simon B, Kuhnle S *et al*. Inhibition of mitochondrial ATP generation by nitric oxide switches apoptosis to necrosis. *Exp Cell Res* 1999; **249**: 396–403.
18. Volbracht C, Leist M, Nicotera P. ATP controls neuronal apoptosis triggered by microtubule breakdown or potassium deprivation. *Mol Med* 1999; **5**: 477–489.
19. Crowe JH, Crowe LM, Oliver AE, Tsvetkova N, Wolkers W, Tablin F. The trehalose myth revisited: introduction to a symposium on stabilization of cells in the dry state. *Cryobiology* 2001; **43**: 89–105.
20. Shaulsky G, Loomis WF. Mitochondrial DNA replication but no nuclear DNA replication during development of *Dictyostelium*. *Proc Natl Acad Sci USA* 1995; **92**: 5660–5663.
21. Fukuzawa M, Araki T, Adrian I, Williams JG. Tyrosine phosphorylation-independent nuclear translocation of a *Dictyostelium* STAT in response to DIF signaling. *Mol Cell* 2001; **7**: 779–788.
22. Fukuzawa M, Abe T, Williams JG. The *Dictyostelium* prestalk cell inducer DIF regulates nuclear accumulation of a STAT protein by controlling its rate of export from the nucleus. *Development* 2003; **130**: 797–804.
23. Zhukovskaya NV, Fukuzawa M, Yamada Y, Araki T, Williams JG. The *Dictyostelium* bZIP transcription factor DimB regulates prestalk-specific gene expression. *Development* 2006; **133**: 439–448.
24. Huang E, Blagg SL, Keller T, Katoh M, Shaulsky G, Thompson CR. bZIP transcription factor interactions regulate DIF responses in *Dictyostelium*. *Development* 2006; **133**: 449–458.
25. Eichinger L, Pachebat JA, Glockner G, Rajandream MA, Sucgang R, Berriman M *et al*. The genome of the social amoeba *Dictyostelium discoideum*. *Nature* 2005; **435**: 43–57.
26. Killick KA, Wright BE. Multiple forms of glucokinase from *Dictyostelium discoideum*. *J Bacteriol* 1978; **133**: 1039–1041.
27. Gottlob K, Majewski N, Kennedy S, Kandel E, Robey RB, Hay N. Inhibition of early apoptotic events by Akt/PKB is dependent on the first committed step of glycolysis and mitochondrial hexokinase. *Genes Dev* 2001; **15**: 1406–1418.
28. Pastorino JG, Shulga N, Hoek JB. Mitochondrial binding of hexokinase II inhibits Bax-induced cytochrome *c* release and apoptosis. *J Biol Chem* 2002; **277**: 7610–7618.
29. Daniai NN, Gramm CF, Scorrano L, Zhang CY, Krauss S, Ranger AM *et al*. BAD and glucokinase reside in a mitochondrial complex that integrates glycolysis and apoptosis. *Nature* 2003; **424**: 952–956.
30. Zaid H, Abu-Hamad S, Israelson A, Nathan I, Shoshan-Barmatz V. The voltage-dependent anion channel-1 modulates apoptotic cell death. *Cell Death Differ* 2005; **12**: 751–760.
31. Nutt LK, Margolis SS, Jensen M, Herman CE, Dunphy WG, Rathmell JC *et al*. Metabolic regulation of oocyte cell death through the CaMKII-mediated phosphorylation of caspase-2. *Cell* 2005; **123**: 89–103.
32. Le Goffe C, Vallette G, Charrier L, Candelon T, Bou-Hanna C, Bouhours JF *et al*. Metabolic control of resistance of human epithelial cells to H₂O₂ and NO stresses. *Biochem J* 2002; **364** (Part 2): 349–359.
33. Richards TA, Cavalier-Smith T. Myosin domain evolution and the primary divergence of eukaryotes. *Nature* 2005; **436**: 1113–1118.
34. Golstein P, Kroemer G. Redundant cell death mechanisms as relics and backups. *Cell Death Differ* 2005; **12** (Suppl 2): 1490–1496.
35. Otto GP, Wu MY, Kazgan N, Anderson OR, Kessin RH. *Dictyostelium* macroautophagy mutants vary in the severity of their developmental defects. *J Biol Chem* 2004; **279**: 15621–15629.
36. Chautan C, Chazal G, Cecconi F, Gruss P, Golstein P. Interdigital cell death can occur through a necrotic and caspase-independent pathway. *Curr Biol* 1999; **9**: 967–970.
37. Roisin-Bouffay C, Luciani MF, Klein G, Levraud JP, Adam M, Golstein P. Developmental cell death in *Dictyostelium* does not require paracaspase. *J Biol Chem* 2004; **279**: 11489–11494.
38. Leist M, Jaattela M. Four deaths and a funeral: from caspases to alternative mechanisms. *Nat Rev Mol Cell Biol* 2001; **2**: 589–598.
39. Sussman M. Cultivation and synchronous morphogenesis of *Dictyostelium* under controlled experimental conditions. In: Spudich JA (ed). *Methods in Cell Biology*. Harcourt Brace Jovanovich: New York, 1987, pp. 9–29.
40. Kay RR. Cell differentiation in monolayers and the investigation of slime mold morphogens. In: Spudich JA (ed). *Methods in Cell Biology*. Ac. Press: Orlando, FL, 1987, pp. 433–448.

Supplementary Information accompanies the paper on Cell Death and Differentiation website (<http://www.nature.com/cdd>)